Nevertheless, it is clear that more information is needed on the size and concentration and the spatial and temporal concentration profiles of ultrafine metal particles.

Ultrafine metals are produced by a wide variety of anthropogenic activities and emitted into the ambient air. Ambient concentrations of such metals have been seen not only in urban settings but also at the cleanest sites in the United States. Concentrations are highly variable as a function of site and time. While ultrafine metals have been seen to persist for many hours, or more, in the clean, dry environment of the arid west, they appear to be rapidly transformed into the accumulation mode in polluted urban or humid rural sites.

6.10 FINE AND COARSE PARTICULATE MATTER TRENDS AND PATTERNS

Data for characterizing PM_{10} are available from a number of AIRS sites across the country. However, data for characterizing $PM_{2.5}$ and $PM_{(10-2.5)}$ as well as PM_{10} are not readily available. As discussed in 6.3.1.7, data for $PM_{2.5}$ and $PM_{(10-2.5)}$ have been obtained at sites in the IMPROVE/NESCAUM networks. However, these sites are located in uninhibited areas. Measurements suitable for determining trends and patterns of $PM_{2.5}$ and $PM_{(10-2.5)}$ in populated areas are available from only a few sites.

Most such data have been obtained with dichotomous samplers which measure $PM_{2.5}$ (an indicator of fine mode particles) and $PM_{(10-2.5)}$ (an indicator of the coarse fraction of PM_{10}). These two fractions may be added together to give PM_{10}. $PM_{2.5}$ is sometimes referred to as fine and $PM_{(10-2.5)}$ as coarse although it is understood that $PM_{2.5}$ will contain that fraction of the coarse mode PM below 2.5 μm diameter and neither PM_{10} nor $PM_{(10-2.5)}$ will contain that portion of the coarse mode above 10μm diameter. Sources of $PM_{2.5}$ (fine) and $PM_{(10-2.5)}$ (coarse) data include EPA's Aerometric Information Retrieval System (AIRS) (AIRS, 1995), IMPROVE (Eldred and Cahill, 1994; Cahill, 1996), The California Air Resources Board (CARB) (CARB, 1995), the Harvard Six-Cities Data Base (Spengler et al., 1986b; Neas, 1996), and the Harvard Philadelphia Data Base (Koutrakis, 1995). The Inhalable Particulate Network (IPN) (IPN, 1985; Rodes and Evans, 1982) provides TSP, PM_{15} and $PM_{2.5}$ data with only a small amount of PM_{10} data.

Data suitable for characterizing the daily variability in $PM_{2.5}$ and PM_{10} are available from only one site in southwestern Philadelphia. The National Weather Service provides daily

observations of visual range, which when suitably treated, can provide an indication of fine mode particle concentration. The Harvard Six Cities study obtained data for $PM_{2.5}$ and PM_{15} every other day for several years. The California Air Resources Board operates about twenty sites that collect $PM_{2.5}$ and $PM_{(10-2.5)}$ data with a sampling frequency of every sixth day. Every sixth day data for a few sites may be found in AIRS. Because of the small number of data sets for $PM_{2.5}$ and either $PM_{(10-2.5)}$ or PM_{10} levels detailed intercomparisons of the behavior of these aerosol size fractions in different regions of the United States cannot yet be made. Data for characterizing the daily and seasonal variability of $PM_{2.5}$, $PM_{(10-2.5)}$, and PM_{10} will be discussed in 6.10.1, the longer term variability (i.e., trends) of $PM_{2.5}$, $PM_{10-2.5}$, and PM_{10} will be discussed in 6.10.2, and the interrelations and correlations among the various PM components and parameters will be discussed in 6.10.3.

The results presented in this section were derived from data bases available to the public. Except for the visibility and National Park trend data, the results presented in this section were prepared for this Criteria Document and have not yet been published elsewhere.

6.10.1 Daily and Seasonal Variability in $PM_{2.5}$ and PM_{10}

In addition to considering patterns of seasonal variations over broad geographical areas, a great deal of information, useful for relating ambient concentrations to health effects, can be obtained by analyzing long time series of concentration data at a single site. Collocated 24-hour $PM_{2.5}$ and PM_{10} filter samples were collected at a site in southwestern Philadelphia from May 1992 through April 1995 (Koutrakis, 1995). This unique data set was collected on a nearly daily basis, thereby allowing an assessment of day-to-day variability in aerosol properties.

The data are presented as box plots showing the lowest, lowest tenth percentile, lowest quartile, median, highest quartile, highest tenth percentile, and highest $PM_{2.5}$ values in Figure 6-101. The four three-month averaging periods shown (March-May, June-August, September-November, December-February) correspond to the so-called climatological or meteorological seasons. Highest median (20.8 $\mu g/m^3$) and extreme (72.6 $\mu g/m^3$)

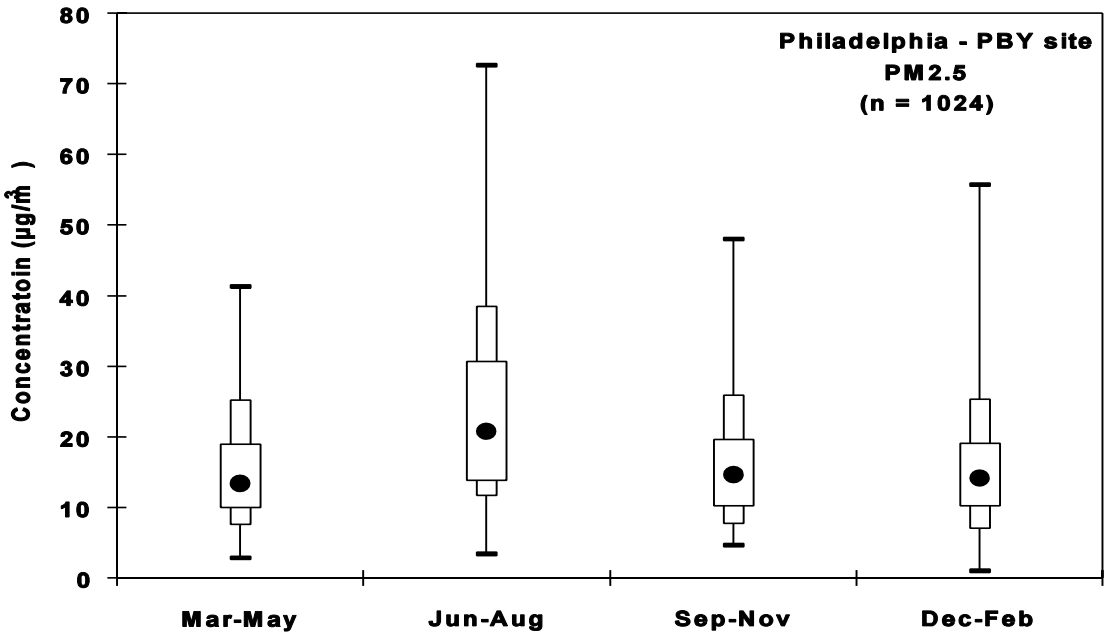

Figure 6-101. Concentrations of $PM_{2.5}$ measured at the PBY site in southwestern Philadelphia. The data show the lowest, lowest tenth percentile, lowest quartile, median (black circles), highest quartile, highest tenth percentile, and highest $PM_{2.5}$ values.

$PM_{2.5}$ concentrations were found during summer, with a difference of 50 µg/m^3 between them. Median $PM_{2.5}$ concentrations are 14.6, 14.2, and 13.4 µg/m^3 for the three quarterly periods from September through May, while maximum concentrations ranged from 41 to 55 µg/m^3. Corresponding PM_{10} data are shown in Figure 6-102. PM_{10} concentrations exhibit strong maxima during both the summer (82.4 µg/m^3) and winter (77.5 µg/m^3). Maximum PM_{10} concentrations during spring and fall are 54.7 and 58.5 µg/m^3. The difference between median and maximum values was 54.4 µg/m^3 during summer and 58.3 µg/m^3 during winter. The median PM_{10} concentration was 28.0 µg/m^3 in summer, and ranged between 19.2 and 20.9 µg/m^3 during the other seasons.

$PM_{2.5}$ and PM_{10} concentrations were highly correlated (r=0.92). PM_{10} and $PM_{(10-2.5)}$ concentrations were less highly correlated (r=0.63) and $PM_{2.5}$ and $PM_{(10-2.5)}$ concentrations were even less well correlated (r=0.30). The day-to-day difference in $PM_{2.5}$ concentrations was 6.8 ± 6.5 µg/m^3 and the maximum difference was 54.7 µg/m^3, while the day-to-day

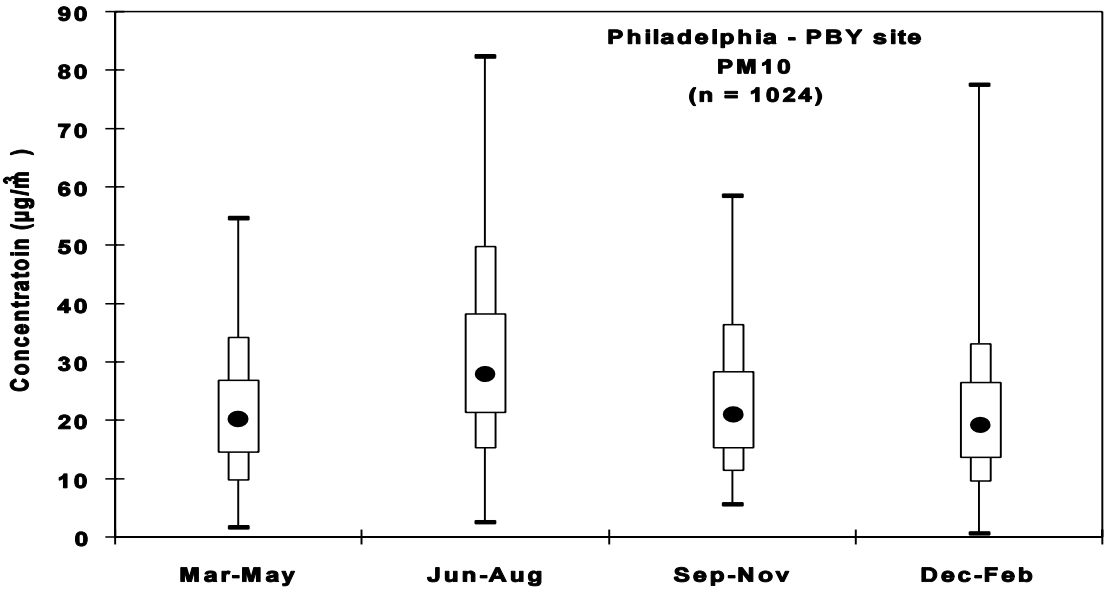

Figure 6-102. Concentrations of PM_{10} measured at the PBY site in southwestern Philadelphia. The data show the lowest, lowest tenth percentile, lowest quartile, median (black circles), highest quartile, highest tenth percentile, and highest $PM_{2.5}$ values.

difference in PM_{10} concentrations was 8.6 ± 7.5 µg/m^3 with a maximum difference of 50.4 µg/m^3. The day-to-day difference in $PM_{(10-2.5)}$ concentrations was 3.7 ± 3.5 µg/m^3 with a maximum difference of 35.1 µg/m^3. The ratio of $PM_{2.5}$ to PM_{10} throughout the measurement period was 0.71 ± 0.13. The high correlation coefficient between $PM_{2.5}$ and PM_{10} along with the high ratio of $PM_{2.5}$ to PM_{10} suggests that variability in $PM_{2.5}$ was driving the variability in PM_{10} levels.

Frequency distributions for the entire three-year $PM_{2.5}$, $PM_{(10-2.5)}$, and PM_{10} data sets are shown in Figures 6-103, 6-104, and 6-105, respectively. Concentrations predicted from the log-normal distribution, using mean values and geometric standard deviation derived from the data, are also shown. The small number of apparently negative $PM_{(10-2.5)}$ values reflects measurement error at low concentration levels. Frequency distributions of aerosol concentrations at several sites in the South Coast Air Basin (Kao and Friedlander, 1995) have also been shown to be reasonably approximated by log-normal distributions.

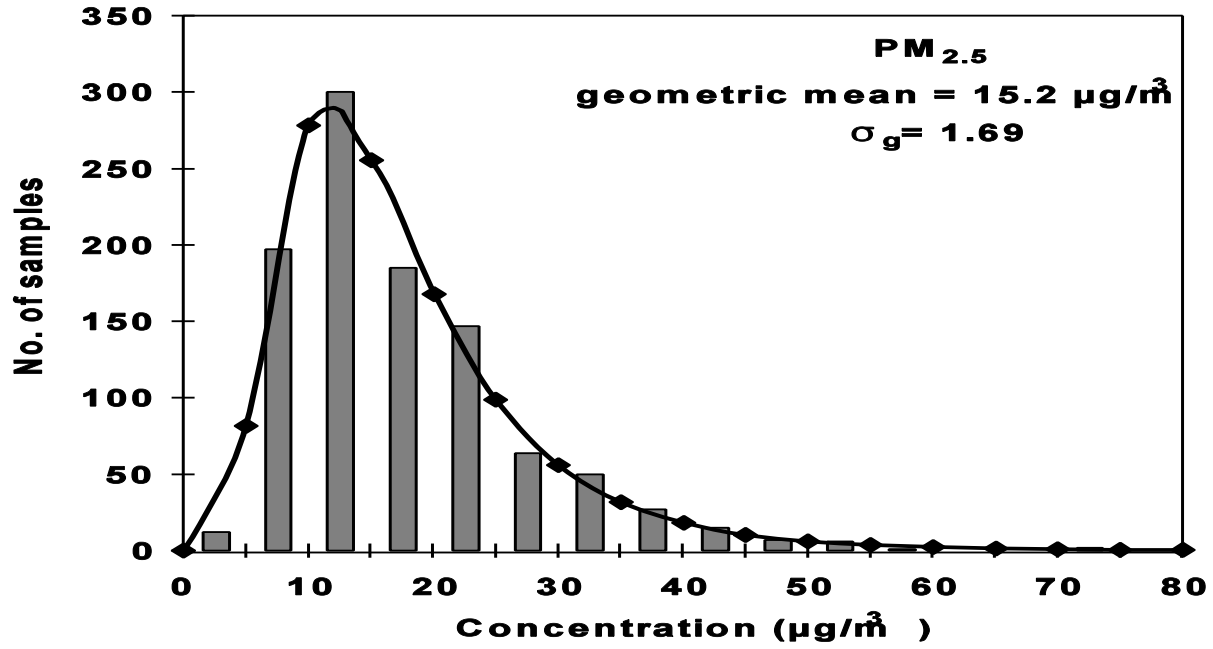

Figure 6-103. Frequency distribution of $PM_{2.5}$ concentrations measured at the PBY site in southwestern Philadelphia. Log-normal distribution fit to the data shown as solid line.

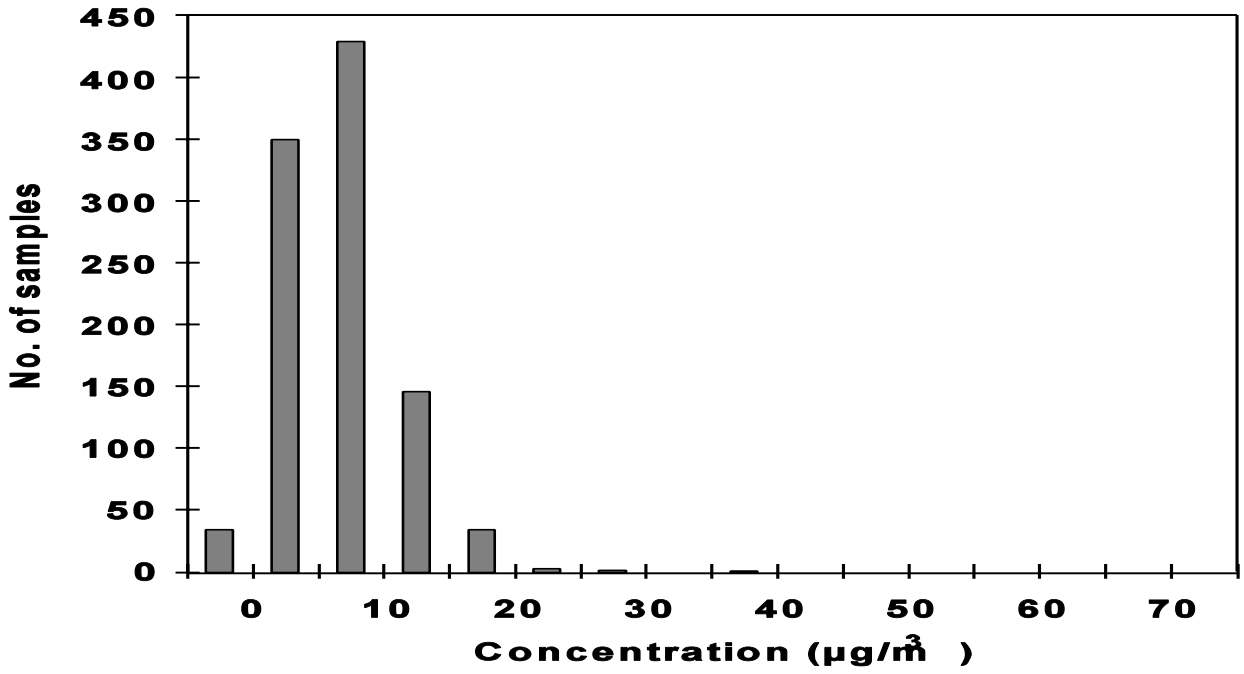

Figure 6-104. Frequency distribution of coarse mode mass derived by difference between PM_{10} and $PM_{2.5}$. Log-normal distribution not shown because of derivative nature of entries.

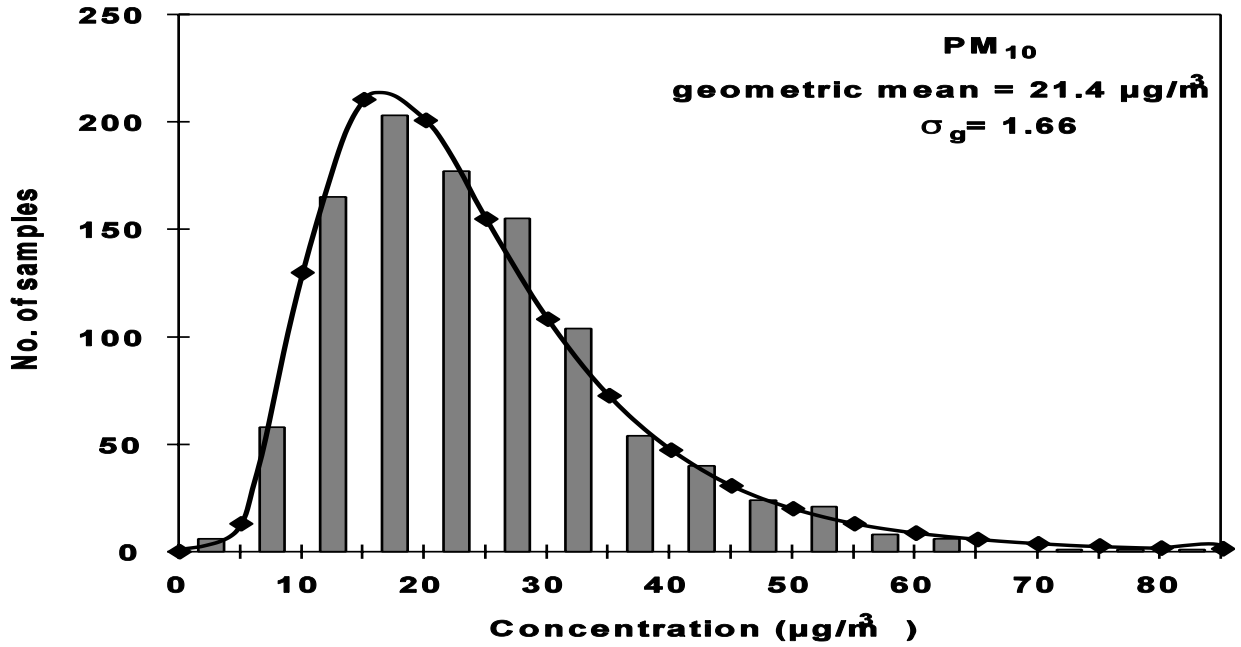

Figure 6-105. Frequency distribution of PM_{10} concentrations measured at the PBY site in southwestern Philadelphia. Log-normal distribution fit to the data shown as solid line.

In general, the highest $PM_{2.5}$ values are observed when winds are from the southwest during sunny but hazy high presure conditions. In contrast, the lowest values are found after significant rainstorms during all seasons of the year. The highest $PM_{2.5}$ values were observed during episodes driven by high sulfate abundances and are due, at least partly, to higher sulfate concentrations. Correlation coefficients between $SO_4^=$ and $PM_{2.5}$ were 0.97 during the summer of 1993. Similar correlations between $SO_4^=$ and $PM_{2.5}$ were found at a site in northeastern Philadelphia (24 km distant from the site under discussion) during the summer of 1993. In addition, $PM_{2.5}$ was found to be stongly correlated ($r > 0.9$) between seven urban sites and one background site (Valley Forge, PA) during the summer of 1993 (Suh et al., 1995). The same relations were also found during the summer of 1994 at four monitoring sites as part of a separate study (Pinto et al., 1995). The results from these studies strongly suggest that $PM_{2.5}$ and $SO_4^=$ concentrations are spatially uniform throughout the Philadelphia area, and that variablility in PM_{10} levels is caused largely by variability in $PM_{2.5}$ (Wilson and Suh, 1996). However, not enough data are available from regional sites to define the total areal extent of the spatial

homogeneity observed in the urban concentrations.

Different conclusions could be drawn about data collected elsewhere in the United States. $PM_{2.5}$ and $PM_{(10-2.5)}$ data were obtained at a number of sites in California on a sampling schedule of every six days with dichotomous samplers (California Air Resources Board, 1995). As an example, frequency distributions of $PM_{2.5}$, $PM_{(10-2.5)}$, and PM_{10} concentrations (calculated as the sum of $PM_{2.5}$ and $PM_{(10-2.5)}$) obtained at Riverside-Rubidoux from 1989 to 1994 are shown in Figures 6-106, 6-107, and 6-108, respectively. It can be seen that the data cannot be satisfactorily fit by a single function, mainly as the result of the complexity of the concentration distribution of the coarse size mode shown in Figure 6-107.

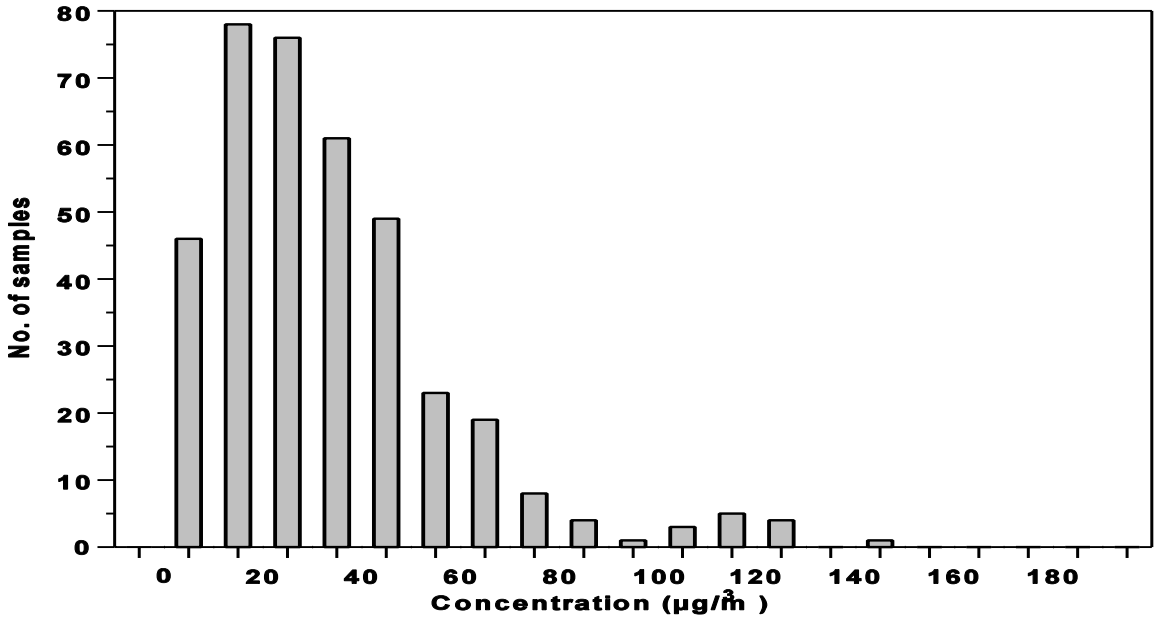

Figure 6-106. Frequency distribution of $PM_{2.5}$ concentrations measured at the Riverside-Rubidoux site.

The data are also presented as box plots showing the lowest, lowest tenth percentile, lowest quartile, median, highest quartile, highest tenth percentile, and highest $PM_{2.5}$ values in Figure 6-109 for four three-month averaging periods (January-March, April-June,

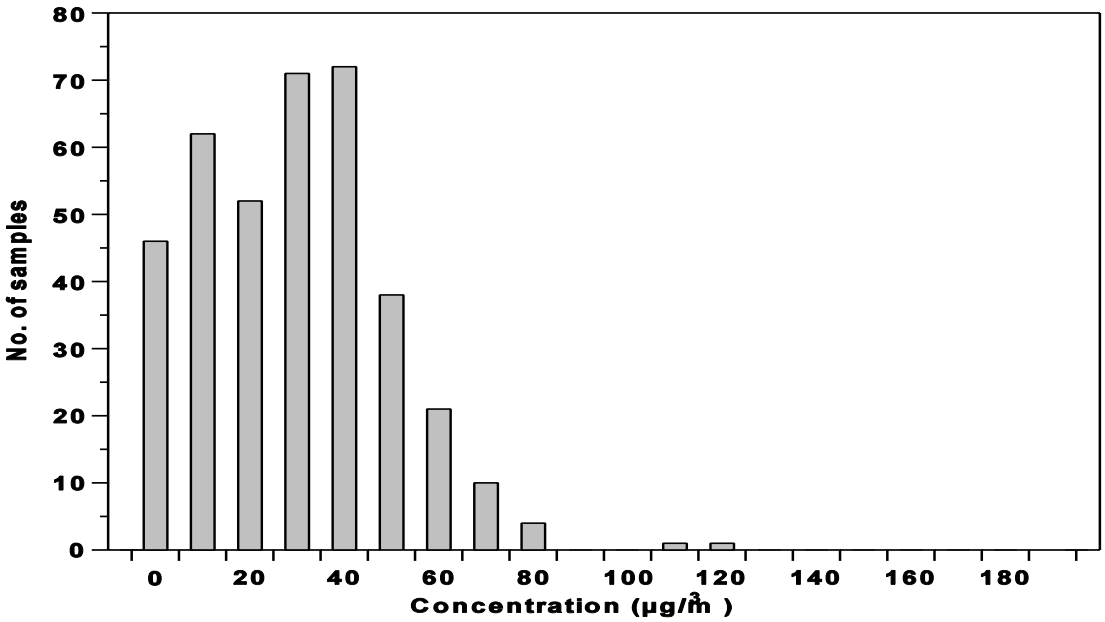

Figure 6-107. Frequency distribution of $PM_{(10-2.5)}$) concentrations measured at the Riverside-Rubidoux site.

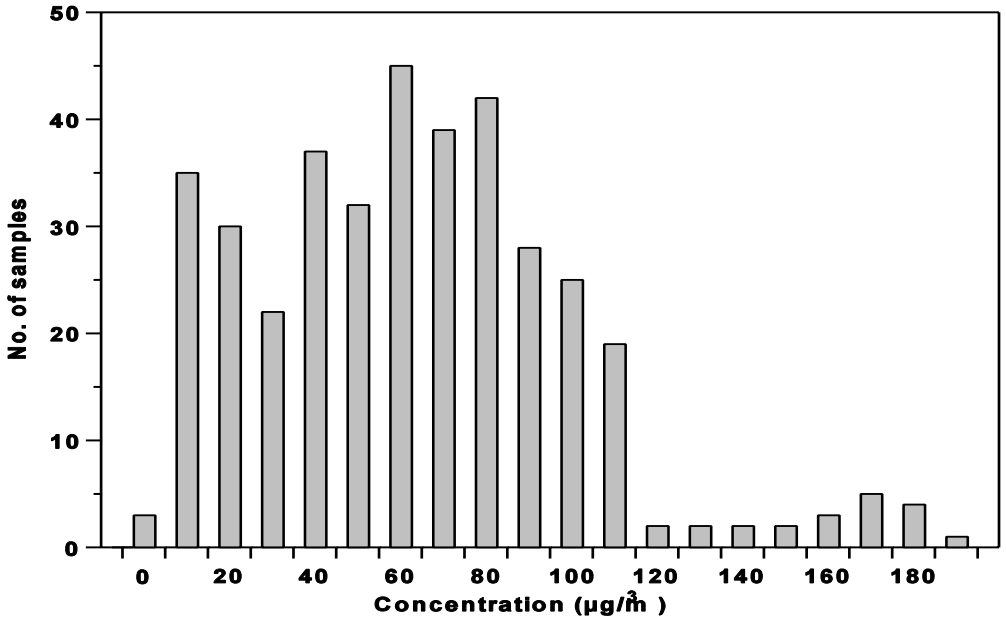

Figure 108. Frequency distribution of PM_{10} concentrations calculated as the sum of $PM_{2.5}$ and $PM_{(10-2.5)}$ masses measured at the Riverside-Rubidoux site.

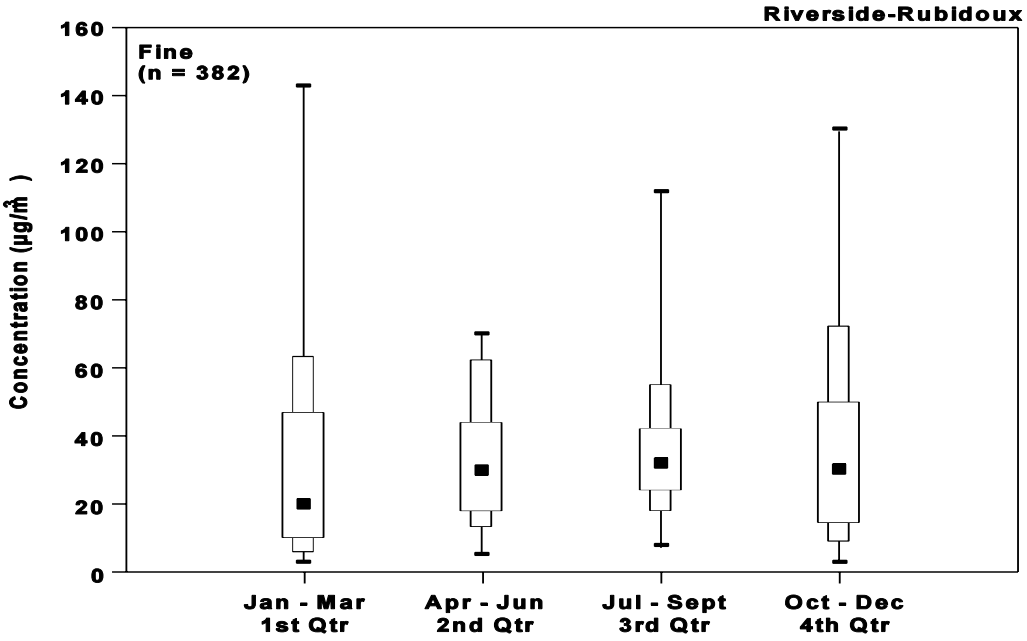

Figure 6-109. Concentrations of $PM_{2.5}$ measured at the Riverside-Rubidoux site. The data show the lowest, lowest tenth percentile, lowest quartile, median (black squares), highest quartile, highest tenth percentile, and highest $PM_{2.5}$ values.

July-September, October-December). Data for $PM_{(10-2.5)}$) and reconstructed PM_{10} are similarly plotted in Figures 6-110 and 6-111. As can seen from these figures, variability in concentrations within an averaging period is high. Differences between median and maximum $PM_{2.5}$ levels range from 40 µg/m^3 during the spring to 123 µg/m^3 during the winter, while differences between median and maximum $PM_{(10-2.5)}$) levels range from 23 µg/m^3 during winter to 83 µg/m^3 during summer. Variations in both size fractions combine to yield differences between median and maximum PM_{10} levels ranging between 83 µg/m^3 and 136 µg/m^3. Median $PM_{2.5}$ levels do not show a clear seasonal cycle. However, $PM_{(10-2.5)}$) concentrations show a maximum during the summer which causes a weak maximum in PM_{10} levels. In fact, median $PM_{2.5}$ (30 µg/m^3) and $PM_{(10-2.5)}$ (34 µg/m^3) levels are identical during the spring and fall quarters. The ratio of $PM_{2.5}$ to PM_{10} mass throughout the measurement period was 0.48 ± 0.13 and $PM_{2.5}$ and PM_{10} levels were moderately correlated (r = 0.47).

An examination of the data from Philadelphia, PA and Riverside, CA indicates that substantial differences exist in aerosol properties between widely separated geographic

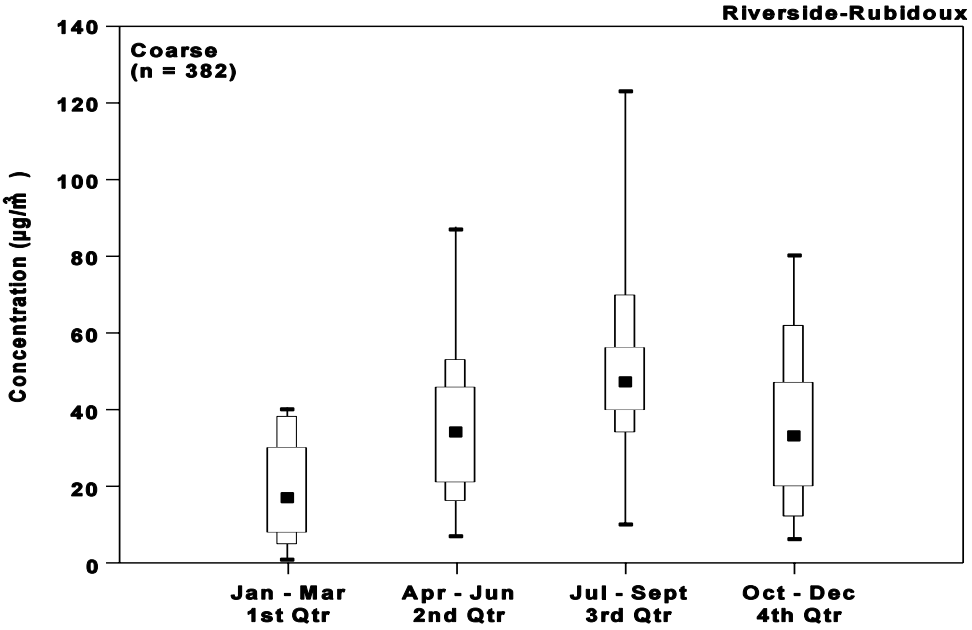

Figure 6-110. Concentrations of $PM_{(10-2.5)}$ measured at the Riverside-Rubidoux site. The data show the lowest, lowest tenth percentile, lowest quartile, median (black squares), highest quartile, highest tenth percentile, and highest PM_{coarse} values.

regions. Fine mode particles make up most of the PM_{10} mass observed in Philadelphia and

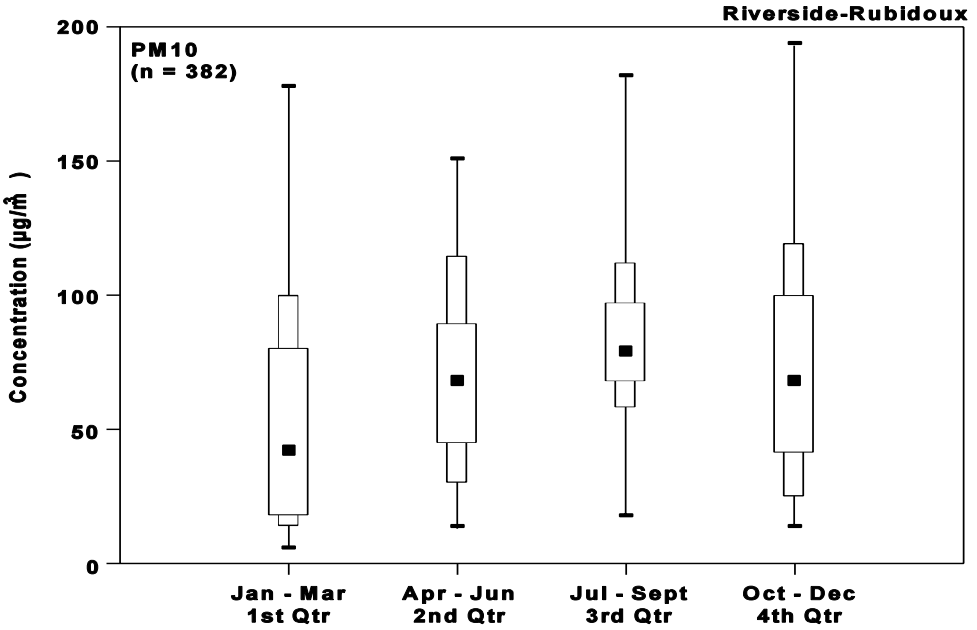

Figure 6-111. Concentrations of PM_{10} measured at the Riverside-Rubidoux site. The data show the lowest, lowest tenth percentile, lowest quartile, median (black squares), highest quartile, highest tenth percentile, and highest PM_{10} values.

appear to drive the daily and seasonal variability in PM_{10} concentrations there. Coarse mode particles are a larger fraction of PM_{10} mass in Riverside and drive the seasonal variability in PM_{10} seen there. The range in the seasonal variation of the ratio of $PM_{2.5}$ to PM_{10} mass is much smaller in Philadelphia (0.70 to 0.75) than in Riverside (0.41 to 0.57) for the four averaging periods used. Differences between median and maximum concentrations in any size fraction are much larger at the Riverside site than at the Philadelphia site. Many of these differences could reflect the more sporadic nature of dust suspension at Riverside. These considerations demonstrate the hazards in extrapolating conclusions about the nature of variability in aerosol characteristics inferred at one location to another.

6.10.2 Fine and Coarse Particulate Matter Trends and Relationships

6.10.2.1 Visual Range/Haziness

Observations of visual range, obtained by the National Weather Service and available through the National Climatic Data Center of the National Oceanic and Atmospheric Administration, provide one of the few truly long-term, daily records of any parameter related to air pollution. After some manipulation, the visual range data may be used as an indicator of fine mode particle pollution. The data reduction process and analyses of resulting trends have been reported by Husar et al. (1994), Husar and Wilson (1993), and Husar et al. (1981).

Visual range i.e., the maximum distance at which an observer can discern the outline of an object, is an understandable and for many purposes an apporpriate measure of the optical environment. It has the disadvantage, however, of being inversely related to aerosol concentration. It is usual, therefore, to convert visual range to a direct indicator of fine mode. particle concentration. The quantitative measure of haziness is the extinction coefficient, B_{ext}, defined as B_{ext}=K/visual range, where K is the Koschmieder constant. The value of K is determined both by the threshold sensitivity of the human eye and the initial contrast of the visible object against the horizon sky. Husar et at. (1994) use K=1.9 in accordance with the data by Griffing (1980). The extinction coefficient is in units of km^{-1} and is proportional to the concentration of light scattering and absorbing aerosols and gases. The radiative transfer characteristics which determine the visual range depend on time of day. Only local noon observations are used.

Haze Trend Summary

The U.S. haze patterns and trends since 1960 are presented in 16 haze maps that represent four time periods and four seasons (Figure 6-112). The selected time periods are 5 year averages centered at 1960, 1970, 1980, and 1990. The quarters are calendrical, i.e., winter is January, February, and March. View horizonally for secular trends by quarter. View vertically for seasonal variation by decade.

The overall national view shows two large contiguous haze regions, one over the eastern U.S. and another over the western Pacific states. The two haze regions are divided by a low-haze territory between the Rocky Mountains and the Sierra-Cascade mountain ranges. This general pattern is preserved over the past 30-year period. However, notable trends have occurred over both the western and eastern haze regions.

The haziness in the western Pacific states covers all of the coastal states, with California having the highest values. In the 1960s a large fraction of western California was very hazy, particularly during Quarters 1 and 4. By the 1990s the magnitude of the Pacific Coast haziness has declined markedly for all seasons.

The eastern haze region extends from the East Coast to the Rocky Mountains. The western boundary of the eastern haze region has been markedly constant over both the seasons and the years. In fact, haze in the mid-section of the U.S., extending from the Rocky Mountains to the Mississippi River, has changed little over the 30-year history.

The most dynamic pattern can be observed over the eastern U.S., extending from the Mississippi River to the East Coast. The eastern U.S. shows a significant seasonal variation. There is also a significant trend over the past 30 years. Furthermore, these seasonal and secular (long-term) trends are different for sub-regions within the eastern U.S., such as the Northeast, Mid-Atlantic and Gulf States regions.

In the 1960s, the highest extinction values were recorded for the cold season (Q1, Q4), with significantly lower values for the warm quarters (Q2, Q3). The remarkable reduction in haziness during the cold season and the strong increase during the warm season has shifted the

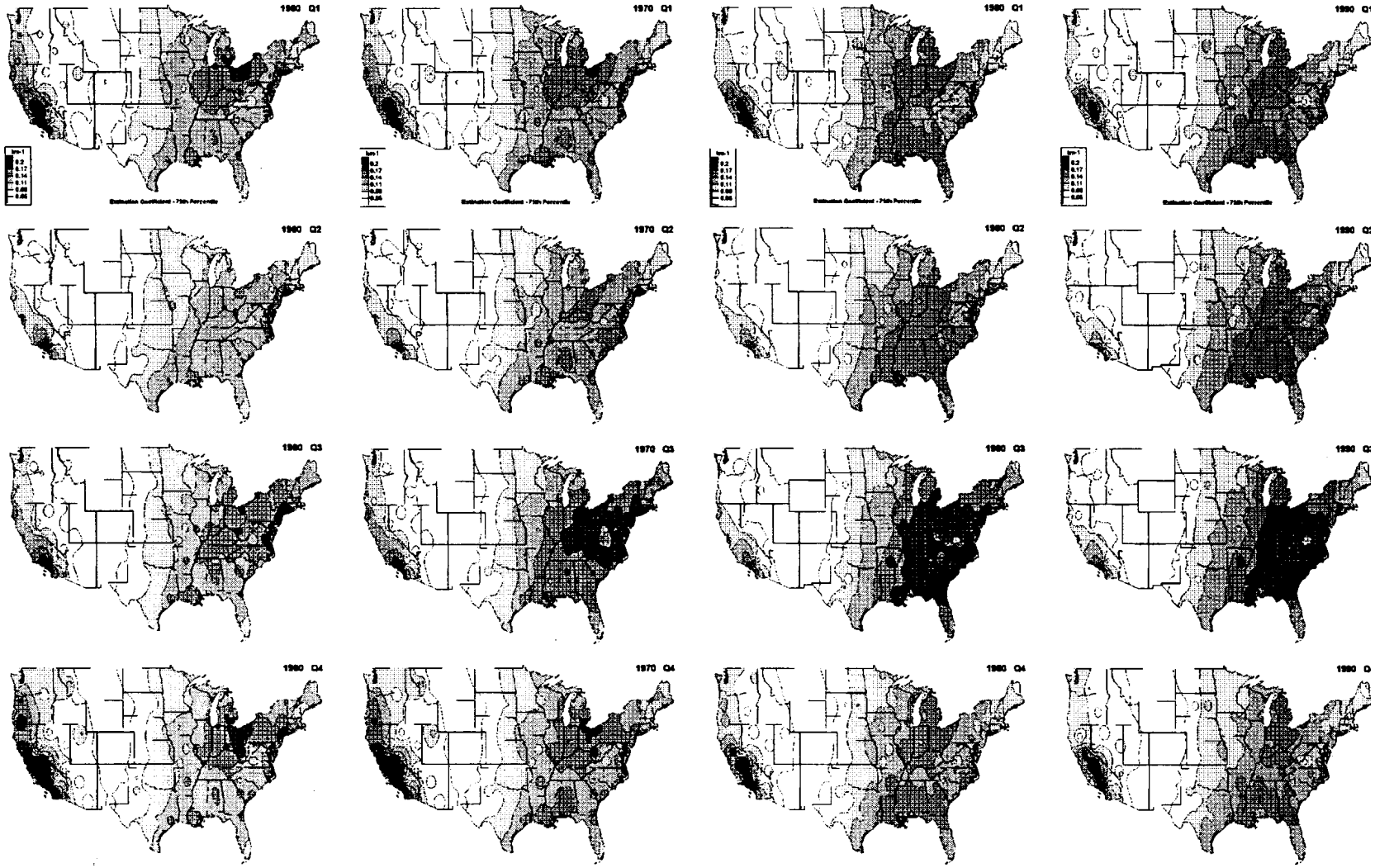

Figure 6-112. United States trend maps for the 75th percentile extinction coefficient, B_{ext} for winter (Q1), spring (Q2), summer (Q3), and fall (Q4). Bext [km^{-1}] is derived from visual range, VR, data by $B_{ext}=1.9/VR$. Data obtained during natural obstructions to vision (i.e., rain, snow, fog) were eliminated.

haze peak from winter to summer. This seasonal change has been accompanied by a regional shift in highest haze pattern. In the 1960s, the worst haziness occurred around Lake Erie and the New York-Washington megalopolis, during the cold season. By the 1990s the area with the worst haze had shifted southward toward Tennessee and Carolinas and occurred in the summer season.

The decade of the 1980s shows less change than the earlier decades. However, there has been a continued haze reduction in the Northeast, north of the Ohio and east of the Mississippi Rivers. The southeastern U.S. as well as the Pacific states remained virtually unchanged in the 1980s.

Regional Pattern

Trends for specific regions in the eastern U.S., and the number and location of visual range reporting stations for each region, are shown in Figure 6-113. The trend graphs represent the 75th percentile of B_{ext} for the stations located within the designated region. The trends are presented for Quarters 1 (winter) and 3 (summer) separately. The northwestern U.S. exhibits an increase of Quarter 3 haze between 1960 and 1970, and a steady decline between 1973 (0.22) and 1992 (0.12). In the winter quarter the haziness has steadily declined from 0.15 to 0.10 in the 30-year period. The Mid-Atlantic region that includes the Virginias and Carolinas shows a strong summer increase between 1960 and 1973, followed by a decline. The winter haze was virtually unchanged over the 30-year period. The haziness over the Gulf states increased between 1960 and 1970, and remained virtually unchanged since then. The central Midwest including Missouri and Arkansas exhibit virtually no change during the winter season and a slight increased in the summer (1960-1970). The upper Midwest (Figure 14) shows an opposing trend for summer and winter. While summer haze has increased, mostly 1960-1973, the winter haze has declined.

6.10.2.2 IMPROVE

The National Park Service-EPA monitoring network for Class I areas is designed to monitor visibility in national parks and other designated areas. Most of these are remote. However, data from two southeastern sites, Shenandoah National Park and the Great Smoky